Available online at www.sciencedirect.com
SCIENCE DIRECT®
ELSEVIER
Nuclear Instruments and Methods in Physics Research B 236 (2005) 1–10
NIM B
Beam Interactions with Materials & Atoms
www.elsevier.com/locate/nimb

Modeling keV particle interactions with molecular and polymeric samples

Arnaud Delcorte *

PCPM, Universite Catholique de Louvain, 1 Croix du Sud, B1348, Louvain-la-Neuve, Belgium

Available online 17 May 2005

Abstract

Organic surfaces are locally submitted to extreme, out of equilibrium conditions when they are bombarded by kiloelectronvolt particles (atoms, ions, clusters). The time scale of the energy transfer is from tens of femtoseconds to several picoseconds depending on the material and the average energy per atom in the energized volume is of the order of a few eV, i.e. sufficient to break bonds in the solid. As a result, atoms, molecules and their fragments are released in the gas phase, which makes sputtering/desorption methods useful for surface treatment (ion beam patterning) and analysis (mass spectrometry). The radicals created in the sample also induce branching and cross-linking reactions that can be useful for surface modification purposes. Molecular dynamics simulations have provided an invaluable help for the elucidation of keV particle-induced processes in organic overlayers and, most recently, bulk materials. In this review, I illustrate the various mechanisms at play using case studies taken from our recent investigations and from the literature. They include the Ar-induced sputtering of a large polymeric molecule on a metal substrate and a molecular sample made of polystyrene oligomers. The emphasis is placed on the understanding of the energy transfer processes in the disturbed surface region and the mechanisms of molecule desorption, fragmentation and recombination, crucial for ion beam-based analytical methods.

PACS: 34.10.+x; 34.20.−b; 34.50.−s; 36.40.Qv; 61.80.Jh; 61.80.Lj; 61.82.Pv; 68.35.Ja; 68.49.−h; 79.20.Ap; 79.20.Rf

Keywords: Sputtering; Particle-induced desorption; Molecular dynamics; Polymer; Molecular solid; Radiation damage; Molecular emission; Secondary ion mass spectrometry

1. Introduction

When a low-energy particle beam interacts with a condensed phase, it creates damage in the surface and triggers the sputtering of atoms, fragments, molecules and/or clusters. The modification

* Tel.: +32 10 473582; fax: +32 10 473452.
E-mail address: delcorte@pcpm.ucl.ac.be

0168-583X/$ - see front matter © 2005 Elsevier B.V. All rights reserved.
doi:10.1016/j.nimb.2005.03.242

induced in organic solid surfaces is beneficial for various applications, including improved metal adhesion [1], biocompatibility [2] and patterning [3]. In addition, the secondary species, intrinsically charged or post-ionized, can be channeled by electric fields through a mass spectrometer for analytical purpose. This principle is used in secondary ion mass spectrometry – SIMS [4,5], secondary neutral mass spectrometry – SNMS [6] and, for analytes dissolved in a liquid organic matrix, liquid SIMS [7] and fast atom bombardment mass spectrometry – FABMS [8,9]. Molecular (multi)layers, biological samples and synthetic polymers constitute an ever-growing field of application for these mass spectrometric techniques.

At the fundamental level, keV projectiles impinging on organic solids and polymers induce a variety of processes [10]. These include chain scissions [11,12], creations of radicals and ions [13], branching and cross-linking reactions [14,15], dehydrogenation [16], sputtering of fragments, chain segments and/or entire molecules [17,18], preferential emission of specific residues [19] and, eventually, carbonization [10]. Analytical models have been developed over the years to describe the energy transfer, damage and sputtering processes associated with the penetration of the projectiles in the matter, mostly for elemental – but sometimes also for organic-samples. Beyond the binary collision (BC) cascade model of Thompson [20] and Sigmund [21], models involving collective atomic motions in the target were proposed to explain the emission of large material clusters in keV and MeV ion bombardment. The rationale is that, after a stage of independent high-energy collisions, well within the BC approximation, the energy dissipation proceeds through large-scale, low-energy, collective motions, and only these collective motions are able to account for the experimental observation of large molecule and cluster emission from surfaces. These early models have been reviewed in previous articles [22–24]. Even though they may successfully delineate general mechanisms, they cannot reproduce the details – and the extent – of the sputtering phenomena in complex, real-world samples.

In this article, I focus on the mechanistic insights provided by classical molecular dynamics (MD), a model that considers an explicit microscopic description of the sample under investigation and predicts the time-evolution of the system – atomic positions and velocities – via numerical integration of the equations of motion. The emphasis is placed on recent studies involving large organic molecules and bulk organic solids. Detailed reviews of the MD studies of sputtering involving hydrocarbon and thiol molecules adsorbed on metals are available elsewhere [25,26].

2. Molecular dynamics and sputtering

A solid sample bombarded by a monatomic projectile evokes a sophisticated pool or marble game [26], at least in the first stage of the process. The successive collisions of the projectile with the atoms of the solid create a first generation of recoil atoms, which, in turn, set a second group of atoms in motion, and so on. At later times, the influence of the bonds in the solid becomes predominant and the system ends up looking like a network of beads interconnected by breakable – and fixable – springs. Sputtering simulations must be able to reproduce both the billiard pool observed at high energy and the beads-and-spring system corresponding to the last, low-energy stages of the interaction. The correct description of bond scission and bond creation processes constitutes another requirement. State-of-the-art molecular dynamics solves these issues using an elaborate toolbox of semi-empirical, often many-body, interaction potentials from which the energy and forces in the system are calculated. These potentials usually blend a strongly repulsive low-distance wall, accounting for the rigid ball behavior in the beginning of the interaction, with a more complex function including a repulsive and an attractive part at larger distance – the springs or glue mimicking the solid behavior in the subsequent stages of the interaction. For instance, in our calculations, the C–C, C–H and H–H interactions are described by the AIREBO potential [27]. This potential is based on the reactive empirical bond-order (REBO) potential developed by Brenner for hydrocarbon molecules [28–30] and includes non-bonding intermolecular interactions through an

adaptative treatment that conserves the reactivity of the REBO potential. At each timestep of the simulation, the forces between the different constituents of the system are calculated from the atomic positions and the interaction potentials. Then Hamilton's equations of motion are integrated to determine the position and velocity of each particle at the following timestep [31,32].

Energy dissipation, damage and sputtering processes in bulk metallic/inorganic samples [33–39] and molecular overlayers on inorganic substrates [25,40] have been thoroughly explored via MD simulations. Bulk-like organic samples have been much less studied, because of their complexity, the scarcity of adequate empirical potentials and the required amount of computer time. Beardmore and Smith modeled a polyethylene crystal under 1 keV Ar bombardment using the aforementioned potential for hydrocarbons, REBO, i.e. without van der Waals interactions between neighboring molecular segments [41]. In more recent reports, the AIREBO potential was used to investigate various organic systems including a benzene crystal [42], benzene multilayers on Ag [43,44], a large (7.5 kDa) polystyrene adsorbate [45,46], kilodalton polystyrene molecules in a low molecular weight matrix [47] and a polystyrene oligomer solid [48]. In contrast with covalently bound polymeric solids, such molecular samples artificially decompose under excitation when intermolecular interactions are not taken into account.

3. Mechanisms of organic sample sputtering

Some of the major features of the interactions between low-energy projectiles and bulk polymeric/molecular samples have been described in [41,42]. First, the projectile breaks bonds in the surface region, creating small fragments that are quickly ejected (in the first hundreds of fs), or transfer their energy to the surrounding medium. In the case of a benzene crystal [42], neighboring molecules are then set in motion without fragmentation, some with an upward momentum. For the polyethylene sample [41], a fraction of the larger fragments created in the target "diffuse" through the solid and escape in the vacuum (between 500 fs and 4 ps).

Fig. 1 illustrates similar observations and complementary aspects of organic sample sputtering using two different hydrocarbon targets. The first one, sample A, is a 7.5 kDa polystyrene (PS) molecule adsorbed on a silver surface [45] and the second, sample B, a molecular solid made of shorter PS oligomers (0.5 kDa) [48]. Frames 1b and 1f describe the trajectories of the Ar projectile and the recoil atoms for the first 150 fs of the considered sputtering events. They provide a view of the atomic collision cascade in the sample, what we called the *collision tree* in a previous article [49]. A few common observations can be made:

- The penetration depth of a 500 eV Ar projectile in a hydrocarbon medium is of the order of 25 Å (which is consistent with calculations of ion range by TRIM [50]).
- Because of the mass ratio between the projectile and the target, the trajectory of the projectile is only slightly deflected by the interactions in the sample, and most of the branches of the tree are forward-directed. This is not the case for Ar atoms impinging on metals [49].
- The projectile and the recoil atoms induce multiple bond scissions in the sample, thereby liberating and transferring a part of their energy to molecular fragments. Some of them will eventually constitute the sputtered flux.
- Only atomic and small molecular ions (C, H, CH, CH_2, C_2H) are emitted in the first 200–300 fs. Larger and more characteristic molecular fragments (C_6H_5 in Fig. 1(c) and C_9H_7 in Fig. 1(d)) are usually desorbed later, after 500 fs.
- Most of the large chain segments (sample A) and intact molecules (sample B) detach from the solid between 3 and 8 ps (Fig. 1(g)).

These results obtained using the AIREBO potential are in broad agreement with those obtained earlier with a polyethylene target and neglecting intermolecular interactions. Nevertheless, for sample A, our detailed results show that introducing intermolecular interactions leads to an average ejected mass per projectile that is twice

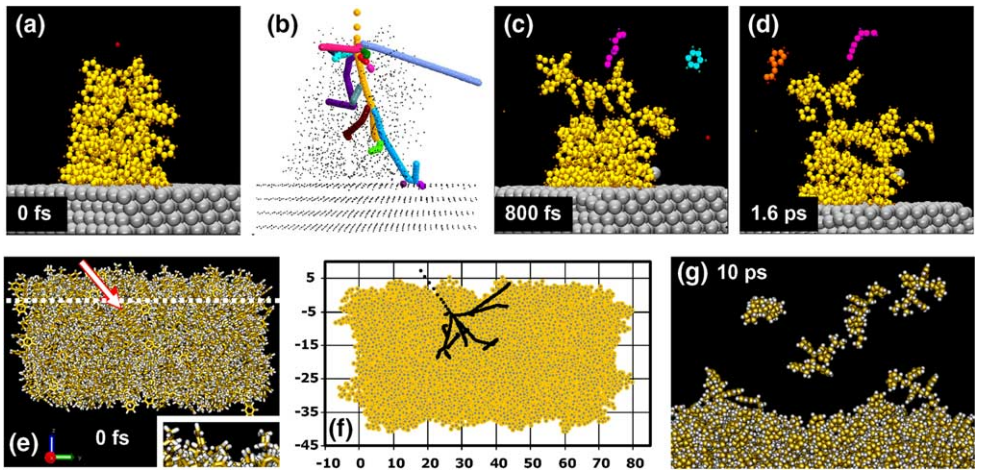

Fig. 1. *Sputtering sample A.* (a) Side view of the computational cell of sample A. The projectile is represented by a red sphere. (b) Collision tree of the atomic collision cascade. (c) and (d) Situation after 800 fs and 1.6 ps. The colored atoms indicate three sputtered PS fragments, including the characteristic C_6H_5 and C_9H_7. Adapted from [45]. *Sputtering sample B.* (e) Side view of the computational cell of sample B. The projectile direction is signified by a white arrow. (f) Collision tree of the atomic collision cascade. (g) Snapshot showing the molecules emitted after 10 ps. Adapted from [48]. (For interpretation of color in this figure legend, the reader is referred to the web version of this article.)

smaller, and a yield of secondary species that is reduced by 25–30% [45]. The same study shows that, for a 7.5 kDa molecule adsorbed on a surface, the large chain segments observed in the sputtered flux come from the top of the molecule, whatever the potential. This observation explains the sensitivity of SIMS to the conformation of large (bio)molecules on the surface [51]. Concerning the timing of the emission, a parallel can be drawn with metal surface sputtering where atoms and small clusters are mainly ejected in the first picosecond while larger chunks of material desorb between 5 and 10 ps [38,39].

A particularly interesting question arises as to what happens in the time gap separating the end of the atomic collision cascade (~100 fs) and the actual desorption of molecular fragments, chain segments and intact molecules. In general, our calculations show that a significant part of the projectile/recoil energy is internalized in the ro-vibrational modes of the molecular species to be desorbed [45–47], the internal energy uptake being, on average, correlated with the size of the fragment [52]. Energy transfer processes are considered in detail hereafter for the case of our PS molecular solid.

4. Energy dissipation and energy localization

To unravel the specific physics related to the penetration of a keV projectile in an organic target, we analyzed the energy transfer/dissipation in the topmost layers of sample B as a function of time [48]. The comparison with a system made of a molecular overlayer physisorbed on a metallic crystal is informative. Fig. 2 gathers the results obtained from the 500 eV bombardment of two samples, the molecular PS solid of Fig. 1(e)–(g) (sample B) and a monolayer of the same PS oligomers on silver (sample L) – see Fig. 2(h) for a top view of the sample [52]. Both events induce the emission of 3 intact PS molecules. The diagrams of Fig. 2 show the cumulated energy of atoms, with an upward momentum, per 5×5 Å^2 surface cell. In the molecular PS sample of Fig. 1(e), the surface layer is defined by the dashed horizontal line. In the monolayer sample of Fig. 2(h), the surface layer consists of Ag, C and H atoms located above the *second* silver plane of the crystal. Note that, because only atoms with an upward momentum are considered, we expect the energy peaks appearing in the diagrams to be correlated with molecular desorption events.

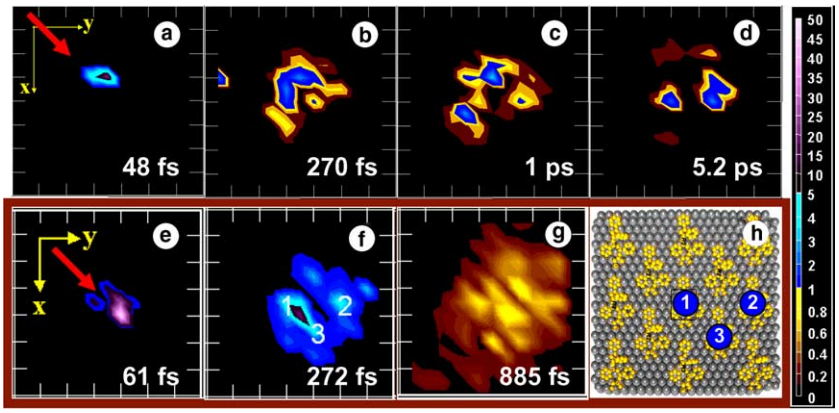

Fig. 2. Time evolution of the kinetic energy distribution in the surface layer of sample B (a)–(d) and sample L (e)–(g) for trajectories inducing the ejection of three intact PS molecules. The frames show the cumulated kinetic energy of atoms with an upward momentum in each 5×5 Å^2 sub-cell of the surface layer, i.e. above the dashed line in Fig. 1(e) (sample B) and above the second layer of Ag atoms in Fig. 2(h) (sample L). The red arrow signifies the direction of the incoming projectile. The numbers (1–3) in frames (f) and (h) indicate the positions of the molecules that are desorbed. The energy scale on the right side of the figure is in eV. Adapted from [48]. (For interpretation of color in this figure legend, the reader is referred to the web version of this article.)

Frames 2a and 2e, before 100 fs, mirror the information given by the collision tree of the events, i.e. only a few atoms are in motion with a relatively large kinetic energy. Beyond this time, the energy dissipates around the "branches" delineated by the trajectories of the projectile and recoil atoms. The comparison between Fig. 2(b)–(d) and (f)–(g) are summarized hereafter:

- Overall, a larger amount of energy is reflected towards the surface, within a shorter time, in the case of the monolayer sample (see Fig. 2(b) and (f)). For the bulk sample (B), the energy remains mostly "trapped" within the molecules that have been excited by the collision cascade and their direct neighbors.
- For sample L, the projectile energy is dissipated across the entire simulation cell within less than 1 ps (see Fig. 2(g)). In sharp contrast, the energy remains localized within a group of surface molecules even beyond 10 ps in the case of the molecular sample (B). (Note that 0.2 eV/sub-cell roughly corresponds to the thermal excitation at ambient temperature.)
- As a result, molecular desorption generally occurs between 300 fs and 2 ps in sample L (molecules 1–3 in Fig. 2(h)) and significantly later in sample B.

The reason for these observations is related to the distinct nature of the samples and, in particular, the potentials at play [48]. In the monolayer sample, the silver crystal mediates the energy transfer and reflection processes. The silver atoms are linked by a network of quite strong, equivalent and non-directional bonds. Therefore, they quickly and easily transfer the received energy among a large group of direct neighbors, which leads to the observed energy delocalization. In addition, the aforementioned mass ratio between the projectile and the silver atoms favors energy reflection towards the surface, if no channeling occurs. In contrast, the bulk PS solid is constituted of two types of bonds, strong inside the molecules (covalence) and weak between the molecules (van der Waals). The energy coupling between these two categories of "springs" is weak and, therefore, the projectile energy is internalized – and tends to remain localized – within the disturbed molecules for a comparatively long time. Rather than a pronounced upward momentum pushing the molecules towards the vacuum [25], it is more the action/reaction between the vibrationally excited surface molecules and their "colder" environment that eventually leads to desorption.

Another important difference is revealed by the statistics of the sputtering events for a large

number of trajectories [48]. While a continuum of events, from low action/low emission (e.g. channeling of the projectile) to megaevents with exceptional emission yields, is observed for monolayers on metal [49] (and metal samples in general), we note that the range of sputtering events appears to be more homogeneous in the case of bulk organic targets. This effect might be due to the amorphous sample structure, preventing the channeling of the projectile.

5. Fragmentation, recombination and cluster emission

The bond-scissions induced by the projectile and the cascade atoms result in the presence of radicals and molecular fragments in the surface region and deeper in the solid. These fragments can either be emitted, like C_6H_5 and C_9H_7 in Fig. 1(c) and (d), or they can stay in the sample, inside regions where the vibrational energy is large enough for the radicals to react or recombine.

Cluster desorption, recombination during the sputtering process and delayed fragmentation reactions after emission are also observed in the simulations [45,47,48,53]. All these processes are mirrored by the mass distribution of the ejected species (mass spectrum in SIMS). One such calculated mass distribution has been published for the case of PS molecules embedded in a trimethylbenzene matrix [47]. The direct fragmentation of analyte/matrix molecules and the formation of matrix:matrix and analyte:matrix clusters, were clearly indicated by the variety of sputtered species. The high mass region of the distribution, Fig. 3, illustrates the importance of the clustering process for such a molecular sample. Mechanistically, non-covalent clusters emerge from the chunks of material that are released in the late stages of the sputtering event (inset). In addition, extended-time calculations show that the analyte:matrix clusters are metastable and they cool via matrix molecule evaporation over the following 100 ps. On a smaller scale, these observations strongly remind the MALDI desorption process [54,55]. The formation and decay mechanisms of clusters ejected from bombarded organic solids

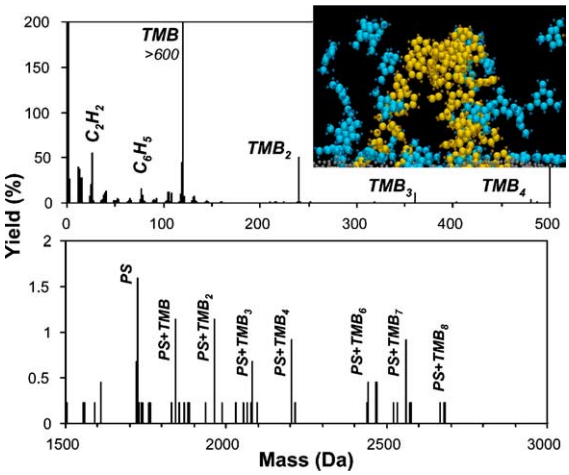

Fig. 3. Mass distribution of fragments, molecules and clusters sputtered from a target made of 2 kDa polystyrene (PS) molecules embedded in a trimethylbenzene (TMB) matrix (after 8.5 ps). Inset: Snapshot showing the desorption of a PS oligomer and several TMB molecules after 3 ps. Adapted from [47].

under particle bombardment also resemble those observed for metal targets [39,56] and thiol overlayers on metals [57]. However, in those systems, the desorption of large-size clusters (>10 metal atoms or 5 constituents in thiol:metal clusters) usually requires a projectile energy over 1 keV and their dissociation, a comparatively larger vibrational excitation, because of the stronger binding between their constituents.

Even though the calculated mass distributions generally reflect the chemical identity of the samples and their fragments, recombination reactions, especially hydrogen transfer/exchange between molecules, are not rare events, e.g. the formation of benzene by addition of H to a detached phenyl. Another example is the observation of H addition to the departing PS molecules in the case of the bulk molecular sample presented in Figs. 1 and 2. For PS molecules with less than 10 eV of internal energy, the adduct H atom attaches in the para position of a phenyl residue, a situation that appears to be energetically favorable for both $R–C_6H_6$ molecules and cations [58]. More complex recombination reactions were observed in the case of the large polymeric molecule, sample A, including the association C_2H_2 with C_7H_5 to form a

C_9H_7 species, but, fortunately for SIMS analysts, such reactions occur in rare occasions and the products usually have a high internal energy, which suggests that they are likely to decompose during their flight time to the detector in an experimental instrument.

The emission depth of molecular species is an important parameter for analytical applications. The simulations of 1 keV Ar bombardment of polyethylene, with a 60° polar incidence angle [41], reveal that H atoms can be sputtered from up to 28 Å below the surface while C atoms originate from the top 16 Å [59]. Our investigations, using 500 eV Ar projectiles directed along the normal of a molecular sample of PS embedded in a matrix, provided values of emission depth that were over 25 Å for H atoms, about 25 Å for C atoms, 20 Å for CH_3 fragments and less than 15 Å for intact trimethylbenzene molecules [47]. They were probably slightly overestimated because of edge effects. For the molecular solid depicted in Fig. 1(e)–(g), under 500 eV Ar bombardment (45° polar angle), most C_2H_2 fragments are sputtered from within the top 20 Å of the surface and all the desorbed intact PS molecule originate from the top 10 Å [48]. The kinetic and internal energies of the molecular fragments are also dependent on their depth of origin, as illustrated in Fig. 4 for acetylene fragments emitted from the same sample (B): there is a clear trend of decreasing kinetic energy with increasing emission depth. A similar trend had been observed for the matrix:analyte sample of [47].

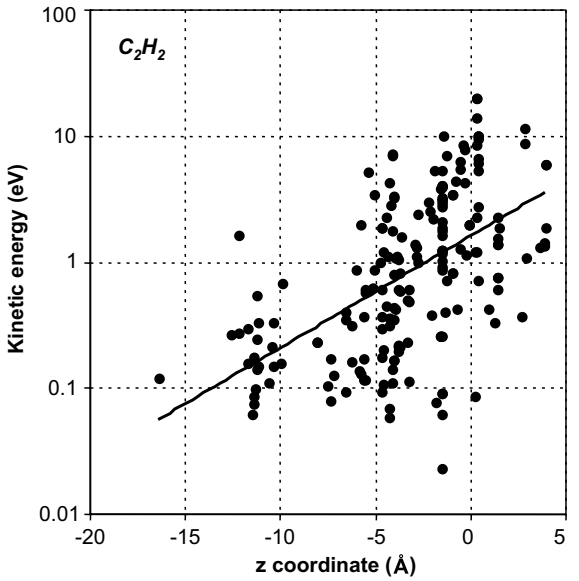

Fig. 4. Plot of the kinetic energy of acetylene molecules sputtered from sample B as a function of their position of origin under the sample surface (+5 Å; see Fig. 1(f)).

6. Ion-induced damage and surface modification

Very few MD studies explicitly consider the damage created in the surface of organic samples under keV particle irradiation. The creation of reactive radicals, inducing further chemical reactions (branching, cross-linking) [41,42,45], is obviously recognized as one source of damage. The formation, per incident particle, of two to three C atoms simultaneously involved in three C–C bonds has been reported for bombarded polyethylene [41]. The bombardment of polyethylene also gives rise to sputtered species with a H:C ratio that is larger than the stoichiometry of the sample (2.66 versus 2.0). This effect should lead to dehydrogenation of the surface, which is experimentally observed for such saturated polyolefins [16]. Preferential dehydrogenation does not occur in our simulations involving polystyrene [48], an unsaturated polyolefin, also in agreement with ion-induced degradation studies of high-molecular weight polystyrene [60]. Note that defect formation/annealing and cross-linking reactions were investigated in detail for the case of carbon nanotubes irradiated by 50–3000 eV Ar [61].

7. Influence of the projectile energy and nature

Most of the MD simulations of organic sample sputtering, including those illustrated above, involve atomic projectiles with sub-keV energies. Some forays into the effects of higher energy projectiles, such as those used in SIMS analysis, indicate that the major fragmentation and emission mechanisms are similar for 500 eV and 5 keV primary Ar atoms [48]. However, on average, the sputtering events affect a larger volume of the

sample, the atomic collision cascades are more developed, and more material is desorbed. An interesting effect favored by higher projectile energies is the overlapping of the collision sub-cascades in a confined nanovolume, inducing collective motion and what appears like a compression wave traveling outwards. In the case of benzene multilayers on Ag, 15 keV Ga and C60 projectiles create a ''splash'' effect in the organic medium, resulting in large emission yields and the formation of a 8 nm/12 nm wide area devoid of molecules in the sample surface [43]. However, the influence of the Ag substrate, in such systems, remains predominant [44]. At this point, it is difficult to predict the specific effects of the nature of the projectile on the sputtering process for organic samples. Preliminary studies using a large benzene crystal, quoted in [43], indicate that 15 keV fullerenes penetrate significantly into the crystal (in contrast with metallic samples), creating an excited volume beneath the surface that subsequently dissipates its energy and ejects molecules via a pressure pulse.

8. Future challenges

In line with the previous discussion, one of the goals for future simulations is the detailed study of the interaction of 5–25 keV monatomic and polyatomic projectiles with molecular samples and polymers. Because this energy range still requires huge samples and intensive computational resources, a rougher description of the system might be much more tractable than the atomistic simulations reviewed in this article (coarse-grained model [62]).

An effort towards modeling more complex organic systems, including various elements (O, N, S) and chemical functionalities is also desirable. Attempts exist in the recent literature for the case of laser-induced desorption of small proteins [63,64] and oligonucleotides [65] from water and organic matrices, but the methods used do not allow for covalent bond-breaking and bond creation, which is inadequate for a correct description of sputtering. Therefore, the design and/or adaptation of appropriate interaction potentials for organic sample sputtering is still an area of development.

An even more challenging issue concerns the simulation of ionization and charge transfer processes occurring in the bombarded solid and in the departing ''plume''. A pioneering study considers the ionization of water molecules/clusters via attachment of alkali metal cation and halogen anions embedded in the ice matrix [66]. A full treatment of ionization and electronic processes, however, introduces another level of complexity. Indeed, because the MD simulations are classical in nature, describing such processes would require the ''artificial'' implementation in the model of ionization/charge exchange probabilities derived from first principle calculations [67], or the first principle calculation of electronic structures, ''on the flight'', for small sub-systems of atoms satisfying some predefined geometric or energetic criteria. Even though such developments constitute real challenges, the recent progress reviewed in this article and the absence of realistic alternative model for organic sample sputtering, show that the future of MD simulations in this area remains promising.

Acknowledgments

I wish to thank Barbara Garrison from the Pennsylvania State University and Patrick Bertrand from the University of Louvain for commenting this manuscript and for their continued support over the years. The financial contributions of the ''Fonds National de la Recherche Scientifique'' of Belgium and the National Science Foundation of America are gratefully acknowledged. Additional computational resources were provided by the Academic Services and Emerging Technologies (ASET) of Penn State University. I am also indebted to the ASET staff for assistance with the Lion-xe and Lion-xl clusters.

References

[1] P. Bodo, J.E. Sundgren, Thin Solid Films 136 (1986) 147.
[2] J.B. Lhoest, J.-L. Dewez, P. Bertrand, Nucl. Instr. and Meth. B 105 (1995) 322.

[3] A. Delcorte, P. Bertrand, E. Wischerhoff, A. Laschewsky, in: A. Benninghoven, P. Bertrand, H.-N. Migeon, H.W. Werner (Eds.), Proceedings of the XII International Conference on Secondary Ion Mass Spectrometry, SIMS XII, Elsevier, Amsterdam, 2000, p. 757.
[4] J.C. Vickerman, D. Briggs (Eds.), ToF-SIMS: Surface Analysis by Mass Spectrometry, SurfaceSpectra/IM Publications, Manchester, 2001.
[5] A. Benninghoven, J.L. Hunter Jr., B.W. Schueler, H.E. Smith, H.W. Werner (Eds.), Proceedings of the XIVth International Conference on Secondary Ion Mass Spectrometry and Related Topics, Appl. Surf. Sci. 231–232 (2004) 1.
[6] C.H. Becker, in: A.W. Czanderna, D.M. Hercules (Eds.), Ion Spectroscopies for Surface Analysis, Plenum Press, New York, 1991, p. 273.
[7] W. Aberth, K.M. Straub, A.L. Burlingame, Anal. Chem. 54 (1982) 2029.
[8] M. Barber, R.S. Bordoli, R.D. Sedgwick, A.N. Taylor, J. Chem. Soc. Chem. Commun. (1981) 325.
[9] M. Barber, R.S. Bordoli, G.J. Elliot, R.D. Sedgwick, A.N. Taylor, Anal. Chem. 54 (1982) 645A.
[10] G. Marletta, Nucl. Instr. and Meth. B 46 (1990) 295.
[11] G.J. Leggett, J.C. Vickerman, Int. J. Mass Spectrom. Ion Processes 122 (1992) 281.
[12] I. Gilmore, M.P. Seah, Surf. Interface Anal. 24 (1996) 746.
[13] J. Sunner, Org. Mass Spectrom. 28 (1993) 805.
[14] A. Licciardello, S. Pignataro, A. Leute, A. Benninghoven, Surf. Interface Anal. 20 (1993) 549.
[15] A. Chilkoti, G.P. Lopez, B.D. Ratner, M.J. Hearn, D. Briggs, Macromolecules 26 (1993) 4825.
[16] A. Delcorte, L.T. Weng, P. Bertrand, Nucl. Instr. and Meth. B 100 (1995) 213.
[17] D.M. Hercules, J. Mol. Struct. 292 (1993) 49.
[18] K. Wien, Nucl. Instr. and Meth. B 131 (1997) 38.
[19] G.J. Leggett, J.C. Vickerman, Anal. Chem. 63 (1991) 561.
[20] M.W. Thompson, Vacuum 66 (2002) 99.
[21] P. Sigmund, in: R. Behrisch (Ed.), Sputtering by Particle Bombardment I, Springer, Berlin, 1981, p. 9.
[22] C.T. Reimann, in: Fundamental Processes in Sputtering of Atoms and Molecules, Matematisk-fysiske meddelelser 43, P. Sigmund (ed.), Det Kongelige Danske Videnskabernes Selskab, Copenhagen, 1993, p. 351.
[23] P. Demirev, Mass Spectrom. Rev. 14 (1995) 279.
[24] A. Delcorte, in: J.C. Vickerman, D. Briggs (Eds.), ToF-SIMS: Surface Analysis by Mass Spectrometry, SurfaceSpectra/IMPublications, Manchester, 2001, p. 161.
[25] B.J. Garrison, A. Delcorte, K.D. Krantzman, Acc. Chem. Res. 33 (2000) 69.
[26] B.J. Garrison, in: J.C. Vickerman, D. Briggs (Eds.), ToF-SIMS: Surface Analysis by Mass Spectrometry, SurfaceSpectra/IMPublications, Manchester, 2001, p. 223.
[27] S.J. Stuart, A.B. Tutein, J.A. Harrison, J. Chem. Phys. 112 (2000) 6472.
[28] D.W. Brenner, Phys. Rev. B 42 (1990) 9458.
[29] D.W. Brenner, J.A. Harrison, C.T. White, R.J. Colton, Thin Solid Films 206 (1991) 220.
[30] D.W. Brenner, O.A. Shenderova, J.A. Harrison, S.J. Stuart, B. Ni, S.B. Sinnott, J. Phys.: Condens. Matter 14 (2002) 783.
[31] D.E. Harrison Jr., CRC Crit. Rev. Solid State Mater. Sci. 14 (1988) S1.
[32] N. Winograd, B.J. Garrison, in: A.W. Czanderna, D.M. Hercules (Eds.), Ion Spectroscopies for Surface Analysis, Plenum Press, New York, 1991, p. 45.
[33] D.E. Harrison Jr., P.W. Kelly, B.J. Garrison, N. Winograd, Surf. Sci. 76 (1978) 311.
[34] R.P. Webb, D.E. Harrison Jr., Phys. Rev. Lett. 50 (1985) 1782.
[35] R. Smith, K. Beardmore, A. Gras-Marti, R. Kirchner, R.P. Webb, Nucl. Instr. and Meth. B 102 (1995) 211.
[36] M.H. Shapiro, T.A. Tombrello, Nucl. Instr. and Meth. B 152 (1999) 221.
[37] M. Kerford, R.P. Webb, Nucl. Instr. and Meth. B 153 (1999) 270.
[38] T.J. Colla, R. Aderjan, R. Kissel, H.M. Urbassek, Phys. Rev. B 62 (2000) 8487.
[39] G. Betz, W. Husinsky, Philos. Trans. Roy. Soc. Lond. A 362 (2004) 177.
[40] M. Kerford, R.P. Webb, Nucl. Instr. and Meth. B 180 (2001) 44.
[41] K. Beardmore, R. Smith, Nucl. Instr. and Meth. B 102 (1995) 223.
[42] K.D. Krantzman, Z. Postawa, B.J. Garrison, N. Winograd, S.J. Stuart, J.A. Harrison, Nucl. Instr. and Meth. B 180 (2001) 159.
[43] Z. Postawa, Appl. Surf. Sci. 231–232 (2004) 22.
[44] Z. Postawa, K. Ludwig, J. Piakowsky, K. Krantzman, N. Winograd, B.J. Garrison, Nucl. Instr. and Meth. B 202 (2003) 168.
[45] A. Delcorte, P. Bertrand, B.J. Garrison, J. Phys. Chem. B 105 (2001) 9474.
[46] A. Delcorte, B. Arezki, P. Bertrand, B.J. Garrison, Nucl. Instr. and Meth. B 193 (2002) 768.
[47] A. Delcorte, B.J. Garrison, J. Phys. Chem. B 107 (2003) 2297.
[48] A. Delcorte, B.J. Garrison, J. Phys. Chem. B 108 (2004) 15652.
[49] A. Delcorte, B.J. Garrison, J. Phys. Chem. B 104 (2000) 6785.
[50] J.P. Biersack, in: P. Mazzoldi, G.W. Arnold (Eds.), Ion Beam Modification of Materials, Elsevier, Amsterdam, 1987, p. 648.
[51] M. Henry, C. Dupont-Gillain, P. Bertrand, Langmuir 19 (2003) 6271.
[52] A. Delcorte, B.G. Segda, B.J. Garrison, P. Bertrand, Nucl. Instr. and Meth. B 171 (2000) 277.
[53] A. Delcorte, B. Arezki, B.J. Garrison, Nucl. Instr. and Meth. B 212 (2003) 414.
[54] L.V. Zhigilei, E. Leveugle, B.J. Garrison, Y.G. Yingling, M.I. Zeitman, Chem. Rev. 103 (2003) 321.
[55] K. Dreisewerd, Chem. Rev. 103 (2003) 395.
[56] A. Wucher, B.J. Garrison, Phys. Rev. B 46 (1992) 4855.
[57] B. Arezki, A. Delcorte, A.C. Chami, B.J. Garrison, P. Bertrand, Nucl. Instr. and Meth. B 212 (2003) 369.

[58] S.G. Lias, J.E. Bartmess, J.F. Liebman, J.L. Holmes, R.D. Levin, W.G. Mallard, J. Phys. Chem. Ref. Data 17 (Suppl. 1) (1988).
[59] R. Smith, S.D. Kenny, D. Ramasawmy, Philos. Trans. Roy. Soc. Lond. A 362 (2004) 157.
[60] A. Delcorte, Undergraduate thesis, University of Louvain, 1993.
[61] A.V. Krasheninnikov, K. Nordlund, Nucl. Instr. and Meth. B 216 (2004) 355.
[62] Y.G. Yingling, B.J. Garrison, J. Phys. Chem. B 108 (2004) 1815.
[63] X. Wu, M. Sadhegi, A. Vertes, J. Phys. Chem. B 102 (1998) 4770.
[64] Y. Dou, N. Winograd, B.J. Garrison, L.V. Zhigilei, J. Phys. Chem. B 107 (2003) 2362.
[65] S. Kristyan, A. Bencsura, A. Vertes, Theor. Chem. Acc. 107 (2002) 319.
[66] I. Wojciechowski, U. Kutliev, S. Sun, Ch. Szakal, N. Winograd, B.J. Garrison, Appl. Surf. Sci. 231–232 (2004) 72.
[67] I. Wojciechowski, A. Delcorte, X. Gonze, P. Bertrand, Chem. Phys. Lett. 346 (2001) 1.